Near-Ground Propagation Measurements for Vehicular Deployments

Dmitrii Solomitckii*, Vasilii Semkin†, Matias Turunen*, Markus Allén*,
Claude Oestges‡, and Mikko Valkama*
* Electrical Engineering Unit, Tampere University, Tampere, Finland,
{dmitrii.solomitckii, matias.turunen, markus.allen, mikko.valkama}@tuni.fi
†VTT Technical Research Centre of Finland Ltd., 02150 Espoo, Finland, vasilii.semkin@vtt.fi
‡ICTEAM, Université catholique de Louvain, 1348 Louvain-la-Neuve, Belgium, claude.oestges@uclouvain.be

***Abstract*—In the nearest future, connected vehicles will be widely spread due to ongoing standardization activities of vehicle-to-everything communications. However, exchanging real-time traffic information is challenging in urban environments with dense traffic where the line-of-sight might be blocked. In this work, we present the measurement results of the automotive communication and radar sensing through the obstructing vehicle, when the transmitting and receiving antennas are located very close to the ground, and the radio waves propagate near-ground, i.e. between the bottom of the car and the road pavement. It is shown that communication between two vehicles is undoubtedly feasible at distances starting from 1.5 m and antenna heights of 0.3 m with 16 dB loss. Almost the same losses are observed in a radar sensing for distances larger than 2 m.**

***Index Terms*—Antenna location, propagation, measurements, V2X communication, radar.**

I. Introduction

The concept of connected vehicles started to be widely exploited in WiFi-based IEEE 802.11p, in order to enable ad-hoc communication and the direct information exchange among vehicles to improve the traffic safety [1]. Later, 3rd Generation Partnership Project (3GPP) proposed the LTE-based vehicular-to-everything (V2X) communication concept, where vehicle-to-vehicle (V2V), vehicle-to-pedestrian (V2P), vehicle-to-infrastructure (V2I) and vehicle-to-network (V2N) were promoted [2]. Such a multi-sided vision helps to improve safety, reduce environmental impact, and increase traffic efficiency. However, LTE-based communication cannot fully meet the requirements on latency and reliability for automotive applications. Therefore, recent 3GPP initiatives have been targeting to combine LTE and 5G New Radio (NR) for V2X to achieve better performance [3]. Within this integration, V2V communication will operate in the millimeter-wave (mmWave) band, and antennas are going to be installed in the front and rear bumpers of a vehicle.

At the same time, standardization activities of the International Telecommunication Union (ITU) resulted in a recommendation [4], where different automotive radars are distinguished by range and resolution but operating in the same mmWave band. Nowadays, the radars are widely installed in luxury and budget vehicles and engaged in Advanced Driver-Assistance Systems (ADAS) [5] such as collision avoidance, night-driving, and cross alerts. Because of similar physical principles and spectral range, the further step of converging radar and communication parts in a single unit is tested by different research groups, e.g. [6]. However, despite the proven feasibility of such combination, the V2V communications and automotive radar exist separately in the standardization documents.

From the operation perspective, automotive radar and communications are only considered in terms of line-of-sight (LOS) operation so far. However, if a vehicle or a building obstruct the LOS link, the information can be forwarded through infrastructure road-side units (RSU), while radar sensing is disabled. At the same time, the simultaneous use of the infrastructure by a large number of vehicles in a traffic jam can potentially lead to resource allocation problems. Thus, the relevant question emerges: *Is there a way to keep the vehicles connected in the LOS-obstructed conditions without infrastructure assistance?* During the ray-tracing simulations in [7], occasionally, it was found that if the transceiver antenna is placed close to the ground, the signal may propagate under the obstructing vehicle and road (waveguide-like propagation) without experiencing much losses. Primarily, this effect might potentially keep the communicating vehicles connected and expand the radar sensing capabilities even in an obstructed LOS scenario. This phenomenon is called *near-ground* propagation, and it is the main focus of this work.

In general, the proposed term is not novel and has already been addressed in several research works. For example, in [8] the investigation of placing a man-portable radio transceiver near ground is presented for military applications. The results of this study show a significant deviation of a signal strength when the position of a soldier is changed. In [9], the authors developed a narrowband radio channel model for ZigBee wireless sensor networks operating in the near-ground conditions. Finally, in [10], authors presented a methodology to model the near-ground short-range propagation loss in forest areas. Nonetheless, in the works mentioned above, the near-ground propagation is not considered for vehicular applications. Therefore, we are aiming to fill this gap by presenting the measurement results and subsequent analysis of near-ground propagation in vehicular deployment, which may

result in developing new technology for V2V communications.

The paper is organized as follows. The measurement setup is presented in Section II. Section III defines the antenna locations and describes the scenario of interest. The results are provided in Section IV, while the conclusions and discussion are in Section V.

II. Measurement Equipment

Two different setups are employed in order to measure the total received power for the communication part and the backscattering power for the radar part. A handheld ultra-portable mmWave spectrum analyzer (SA) Anritsu MS2760A, operating at the carrier frequency of 27.7 GHz acts as a communication receiver. A resolution bandwidth of 100 kHz and a measurement bandwidth of 200 MHz achieves fast sweep time with a displayed average noise level of -55.5 dBm. A coaxial cable with an insertion loss of 8 dB is connected between the SA and Pasternack PE9851A-20 horn antenna. The horn antenna gain is 20 dBi and the half-power beamwidth is 17°. The communication signal is transmitted with the same hardware that is used in the radar setup, which is described in the next paragraph. The transmitted power is 10 dBm.

The radar measurements are carried out with the use of the mmWave radar setup described in [11]. The transmitter (Tx) and receiver (Rx) antennas are spatially separated by 0.1 m to improve the isolation between the transmitting and the receiving chains. An NI PXIe-5840 vector signal transceiver (VST) is used for transmitting and receiving the RF signal at an intermediate frequency (IF) of 3.5 GHz. Two Keysight N5183B signal generators are employed as local oscillators together with external mixers to up/down-convert the IF signal to/from 27.7 GHz carrier frequency. The modulated orthogonal frequency-diversity multiplexing (OFDM) signal with 200 MHz bandwidth and 60 kHz subcarrier spacing is fed to the PE9851A-20 horn antenna. The transmitted power is 10 dBm. An identical receiving antenna is employed to capture the backscattering signal from the driving vehicle, recognized by the Doppler shift. The displayed average noise level is -80.0 dBm. Both antennas are installed at the height of H on the tripods in order to replicate a vehicular radar system mounted on a bumper. For all configurations, a fixed signal duration of 10 ms is considered, which implies the same radar velocity resolution for all cases. Finally, sub-carrier-domain processing algorithms were developed to utilize the transmit and receive grids of samples.

III. Measured Deployments

First, it is necessary to determine the lowest height and place on a typical vehicular body where transmitting and receiving antennas may be installed. Then, we provide a description of the two measurement scenarios, i.e. communication and radar sensing ones.

A. Defining the Antenna Location

Intuitively, the Tx and Rx antenna heights should be as minimal as possible to reduce the car blockage effect and, consequently, let the signal freely propagate in the waveguide-like conditions. At first glance, the hypothetical minimal point for the antenna placement should be related to the ground clearance[1] (dimension a in Fig. 1a). However, in most cases, the ground clearance is formed by the protruding parts of axles, gearbox, drive shaft at which the installation of the antennas seems not realistic. Following this, the geometries of some passenger cars and trucks listed in Tab. I are manually measured to find a suitable area for the antenna placement. The results show that the best-unified antenna location is *the lowest point of the car bumper* at height 0.3 m for cars and 0.5 m for trucks. These two reference values are used further in the measurements, described in Section IV.

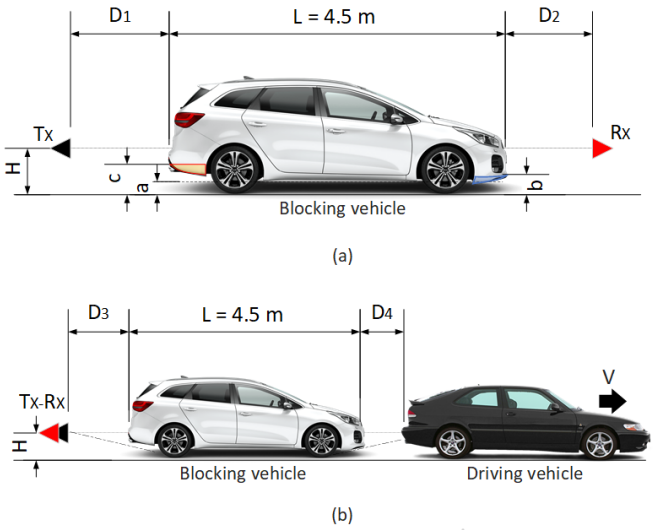

Fig. 1. Measured deployments of near-ground propagation: (a) V2V communication, (b) automotive radar sensing.

TABLE I
Dimensions of Typical Cars

N	Model	a, m	b, m	c, m
1	Kia Ceed (2015)	0.14	0.18	0.27
2	Saab 9-3 Aero (2002)	0.13	0.16	0.23
3	Audi A4 (2018)	0.13	0.17	0.26
4	Mini Cooper (2010)	0.15	0.19	0.24
5	Skoda Octavia (2018)	0.16	0.20	0.27
7	MAN (not identified)	0.25	0.50	0.45
8	SISU (not identified)	0.27	0.45	0.40

The bumper specific heights might be considered, which usually depends on *front* and *rear ground clearance* (dimensions b and c in Fig. 1a) with the range of 0.16–0.27 m for passenger cars and 0.4–0.5 m for trucks. It may seem that such a small difference is negligible. However, as shown in [8] and confirmed in Section IV, the blockage loss strongly depends on the antenna height, and even a few centimeters may be crucial. Thus, in practice, the site-specific heights (blue and red in Fig. 1a) are the places more preferable for the antenna

[1]The distance between the supporting surface (road pavement) and the lowest point of the central part of the car.

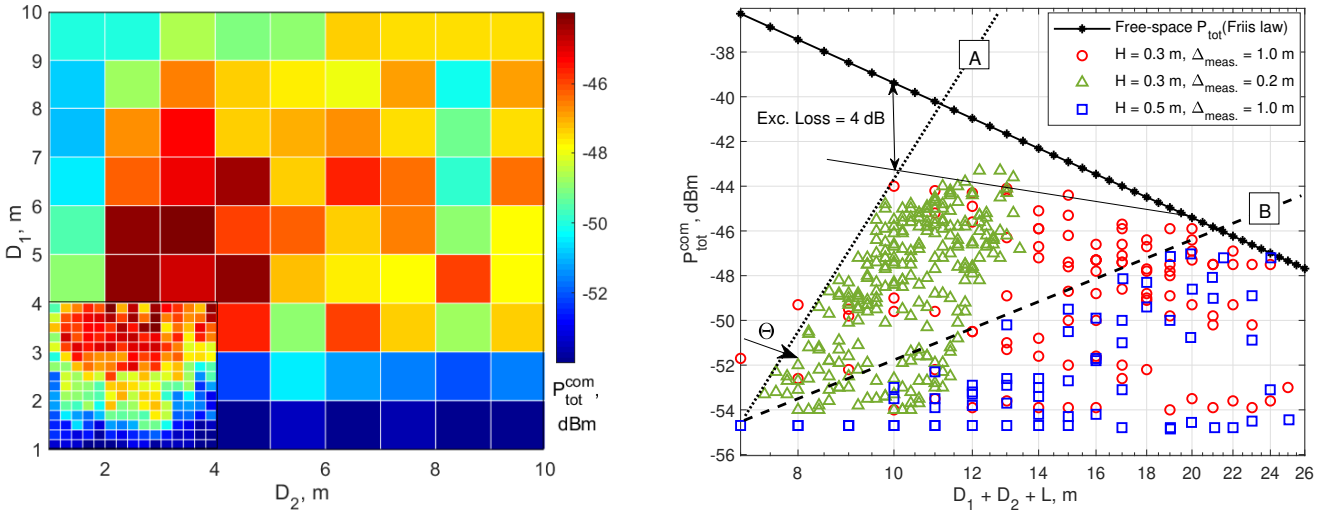

(a) (b)

Fig. 2. (a) Measured total received power as a function of D_1 and D_2 at H = 0.3 m. Small figure precises the measured data in the range D_1 = D_2 = 1–4 m. (b) The measured total received power as a function of D_{sum} = D_1 + $D_2 + L$, where additional measurements at H = 0.5 m are performed.

installation. In this work, we do not consider any antenna position offset and assume that it is installed in the center of the bumper.

B. Scenarios of interest

The measurement results are obtained in the campus of Tampere University (Tampere, Finland). The first deployment is shown in Fig. 1a and presumes the V2V communication between the two vehicles, whose antennas (the black triangle is Tx, the red triangle is Rx in Fig. 1a) are placed at the lowest point of the front and rear bumpers accordingly. However, opposite to the typical V2V scenarios suggested by 3GPP in [3], the blocking car Kia Ceed (white car in Fig. 1a) is introduced between the Tx and Rx antennas to obstruct the LOS link. Furthermore, the antenna height H, as well as inter-vehicular distances from the antennas to the blocking vehicle denoted as D_1 and D_2, are used to characterize the power/loss of near-ground propagation as a function of vehicle type and traffic conditions. Specifically, the antenna heights (H) of 0.3 and 0.5 m refer to the lowest bumper point of a passenger car and a truck (as defined in Section III-A), while the varying values D_1 = D_2 = 1–10 m reflect different traffic situation. For example, the dense traffic jam is characterized by 1 m distance between adjacent vehicles, while the normal traffic conditions in urban scenarios assume to have distance between the vehicles 10 m.

The second measurement scenario demonstrates the functionality of the automotive radar sensing in near-ground conditions with the presence of static blocking car. This scenario does not explore any new capabilities of the automotive radar but extends the existing ones by changing the antenna height. For example, it gives more awareness of the dynamics and the position of vehicles in the traffic flow. Unlike the previously described communication scenario, where antennas are spatially separated, the suggested radar scenario collocates Tx and Rx together, mimicking the operation of typical millimetre-wave automotive radars. Furthermore, in addition to the static blocking vehicle Kia Ceed (white car in Fig. 1b), the driving vehicle Saab 9-3 Aero (black car in Fig. 1b) is introduced. The radar antennas are placed at a certain distance D_3 to the blocking vehicle. Then, on command by the equipment operator, the driving car starts moving from D_4 = 1 to 15 m. The back scattering power is measured 15 times when the driving car moves. The driving speed varies along the trajectory in the range of $v \in [0, 4]$ m/s.

IV. Results

A. Total Received Power for V2V Communication

The main purpose of these measurements is to acquire a relationship between the total received power P_{tot}^{com} and the distances D_1 and D_2 in the deployment shown in Fig. 1a. We evaluate the losses of near-ground propagation in a communication scenario as a function of total distance between Tx and Rx, i.e. D_{sum}= D_1 + $D_2 + L$. To achieve this goal, first, 100 measurements of D_1 = 1–10 m, D_2 = 1–10 m at H = 0.3 m are performed by measuring power with the step of $\Delta_{meas.}$ = 1 m. The obtained results are presented in Fig. 2a. This plot shows that at minimal distances of D_1 or D_2, the received power is very close to the noise level due to blockage by the car's bumper. Meanwhile, the maximum value of P_{tot}^{com} in the region of D_1 or D_2 is equal to 2–3 m, where, the blockage effect may not have an impact anymore. Such behaviour is studied in more details further in this section. It is necessary to say that we performed over 250 additional measurements in the range of D_1 = 1–4 m, D_2 = 1–4 m with step $\Delta_{meas.}$ = 0.2 m. This small region can potentially be of significant interest, as it serves the transient region from strong to weak blockage shown as a sharp difference of P_{tot}^{com} at D_2 = 2 m and D_3 = 3 m in Fig. 2a.

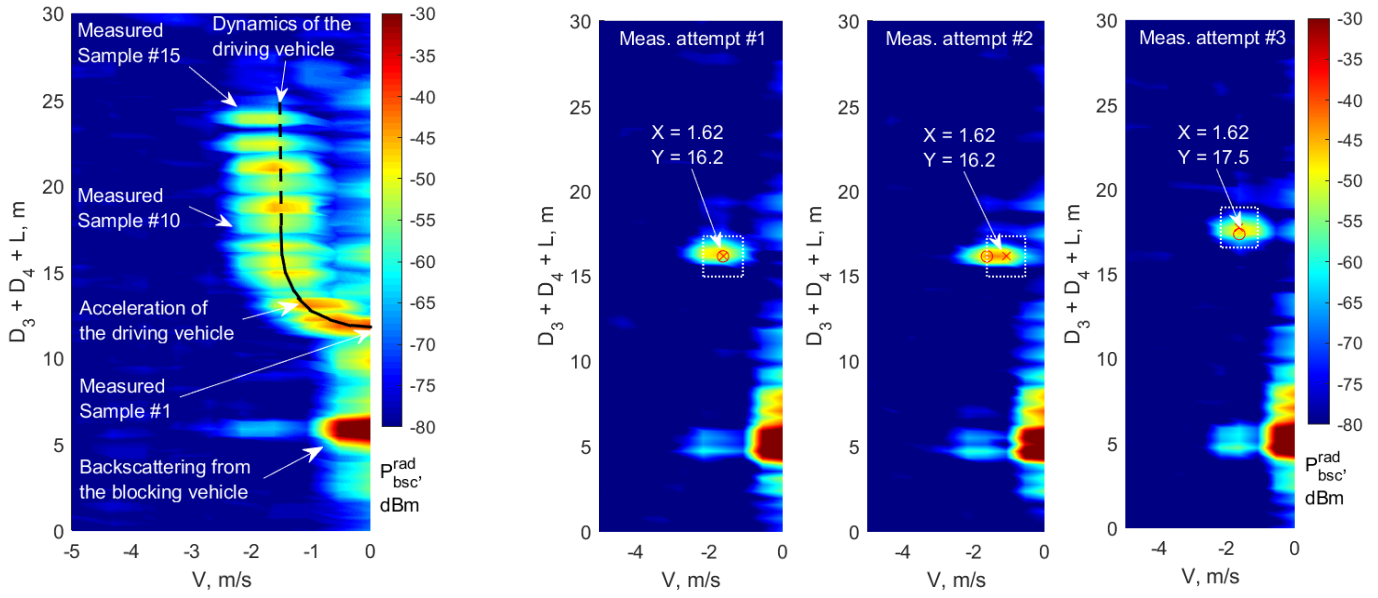

(a) (b)

Fig. 3. The measured backscattering power as a function of D_{sum} = D_3 + $D_4 + L$: (a) 15 overlapped measured samples, (b) three measurement attempts of the same deployment.

The results of these additional measurements are presented in Fig. 2a. First, more precise measurements at $\Delta_{meas.}$ = 0.2 m show that the blockage level is weaker than at $\Delta_{meas.}$ = 1 m, and, indeed, the transition zone is less sharp. Intuitively, the symmetry is expected in Fig. 2a because of the equal distances. However, it does not happen due to different geometry of the front and rear bumpers (see Tab. I). Furthermore, as long as $c > b$ is valid for all vehicles in Tab. I, the blocking effect is more notable for the front bumper than for the rear. It can be observed in Fig. 2a by the wider deep blue region of P_{tot}^{com} along D_2 at D_1 = 1 m.

A two-dimensional plot, comparing the measured total received power with the theoretical Friis law as a function of total distance between antennas D_{sum} = D_1 + D_2 + L is demonstrated in Fig. 2b. The $\Delta_{meas.}$ = 1 m (red) and $\Delta_{meas.}$ = 0.2 m (green) measured data, is plotted in this figure. Additionally, 100 extra measurements of P_{tot}^{com} at H = 0.5 m, D_1 = 1–10 m, D_2 = 1–10 m and step $\Delta_{meas.}$ = 1 m are added in Fig. 2b as blue markers. The introduced line A bounds the red and green data markers, while line B outlines the blue ones. When the Tx and Rx antennas are located close to the blocking car (i.e. D_{sum} = 7 m in Fig. 2b), the signal is quite strongly attenuated by the bumper, and, thus, cannot contribute to the P_{tot}^{com}. The total power received at this distance is -53.8 dBm and corresponding excess loss is 16.5 dB. As the distance D_{sum} increases, the P_{tot}^{com} raises proportionally along the line A, due to the diminishing blockage effect. Apparently, the maximum level of P_{tot}^{com} = -43 dBm is associated with the termination of the bumper blockage and the appearance of a first-order reflection from the ground. Due to the grazing angle of the signal incidence, the losses related to the Fresnel reflection and roughness tends to be zero either. The excess loss at P_{tot}^{com} = -43 dBm is about 3–4 dB. After the maximum is reached, the received power begins to decrease gradually, converging with the Friis law. In turn, the raising of H to 0.5 m (blue squares in Fig. 2b) proportionally increases the level of blockage. In particular, the dashed line B rises slower, than the line A. Oppositely to H = 0.3 m, near-ground transmission does not work at short (D_{sum} = 7–10 m) distances when H = 0.5 m. The first detected P_{tot}^{com} is available only at D_{sum} = 10 m, which corresponds to $D_1 \approx D_2 \approx 2.7$ m.

B. The Back-scattering Power for Radar Sensing

The backscattering power P_{bsc}^{rad} reflecting from the driving vehicle (Saab 9-3 Aero in Fig. 1b) is measured to evaluate the received power and losses for the near-ground radar sensing layout. The distance D_3 has a discrete range from 1 to 5 m with 1 m step, while the D_4 dynamically varies from 1 to 15 m together when the vehicle is driving. When the car starts its movement, the radar setup measures 15 samples. Each of these samples is saved in a separate file, containing the distribution of the backscattering power as a function of speed and total distance D_{sum} = D_3 + $D_4 + L$. For example, Fig. 3a demonstrates the overlay of all 15 measurements in one plot, where the scattering from the driving vehicle is showed along the trajectory of the driving car (black line). The curvature of the trajectory is caused by the acceleration of the driving vehicle from 0 m/s. The large red static spot is created by high-power reflections from the blocking vehicle (in this case Kia Ceed, Fig. 1b).

Three measurement attempts are accomplished for each of the D_3 values, to obtain larger number of the measurement samples. As an example, 3 measuring attempts at a certain D_3 = 5 m and D_3 + $D_4 + L \approx$ 16 m are shown in Fig. 3b. It is visible that the detection (red markers) of P_{bsc}^{rad} in first and second attempts happened almost at the same [X,Y], while the

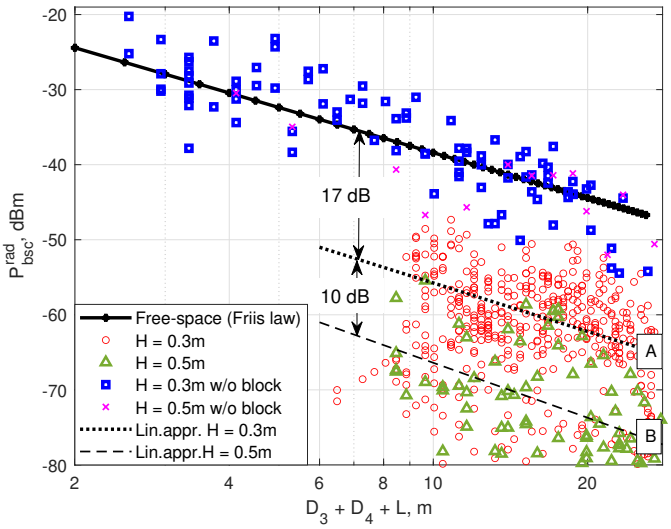

Fig. 4. Back scattering power from the driving vehicle with near-ground propagation as a function of $D_{sum} = D_3 + D_4 + L$.

third attempt is shifted by 1.3 m along the Y. The main reason is different speed of the moving vehicle.

The final step is to obtain the P^{rad}_{bsc} as a function of $D_{sum} = D_3 + D_4 + L$, similarly to Fig. 2b. For this, first, the measurements at $H = 0.3$ m and $H = 0.5$ m are carried out as in Fig. 3b. Additionally, the LOS measurements without the blocking vehicle are performed to successfully calibrate the P^{rad}_{bsc} with the Friis law. Next, the algorithm that searches the maximum measured power of a signal scattering from the driving vehicle at related distance $D_{sum} = D_3 + D_4 + L$ is developed and applied. The results of the algorithm are shown as the red markers in Fig. 3b. The final Fig. 4 is plotted from the processed maximum values at related D_{sum}. Based on this plot, the effect of the antenna height is studied. Specifically, if the antenna is installed at a height of $H = 0.3$ m, the mean excess loss is about 17 dB. Further increasing the height H to 0.5 m, decreases the average power by extra 10 dB. At the same time, strong power fluctuations caused by multipath interference can also be observed over all measured data.

V. Conclusions and Discussion

This paper investigates the concept of near-ground communication and radar sensing for vehicular deployments. The dedicated measurement campaign is performed and the results are analyzed. Total received power for communication part and back scattering power for the radar part were selected as the metrics of interest. Based on the analysis of the measured results the following is observed. First, it can be seen that for the Tx and Rx antenna heights of $H = 0.3$ m, at $D_1 = D_2 =$ 1–1.5 m (corresponds to $D_{sum} =$ 7–7.5 m) the received power is $P^{com}_{tot} = -53$ dBm and excess loss is 16 dB. Second, the radar sensing scenario when the antennas are at $H = 0.3$ m and $D_1 = D_2 =$ 1–1.5 m is questionable due to relatively low received power $P^{rad}_{bsc} = -70$ dBm and corresponding 40 dB excess loss. Such differences may be due to the radar cross-section of the driving car bumper. The radar sensing losses become smaller (10 dB) at $D_{sum} = 9$ m, which corresponds to $D_3 = D_4 = 2.2$ m. In general, increasing the distance between vehicles reduces the losses caused by the bumper blockage. At long distance D_{sum}, the signal freely propagates under the blocking vehicle, and via one reflection can be received by the Rx antenna. Also, varying the antenna height to $H = 0.5$ m has negative impact on the performance of near-ground propagation: communication and radar sensing start operating when the distance between vehicles is about 2.5–3 m. In this case, the received powers are $P^{com}_{tot} = -53$ dBm and the excess loss is about 12 dB, while $P^{rad}_{bsc} = -65$ dBm and corresponding losses are 24 dB.

Acknowledgment

This work was supported in part by the Academy of Finland, grants №319994, №331810 and by the MUSEWINET project under the Belgian Science Foundation FRS-FNRS (Fonds de la Recherche Scientifique) EOS program.

References

[1] D. Jiang and L. Delgrossi, "IEEE 802.11 p: Towards an international standard for wireless access in vehicular environments," in *VTC Spring 2008-IEEE Vehicular Technology Conference*. IEEE, 2008, pp. 2036–2040.

[2] "Study on LTE Support for Vehicle to Everything (V2X) Services. Technical report, Release 14," *3GPP TR 22.885*, Dec. 2015.

[3] "Study on NR Vehicle to Everything (V2X) Services. Technical report, Release 16," *3GPP TR 38.885*, Mar. 2019.

[4] "Systems characteristics of automotive radars operating in the frequency band 76-81 GHz for intelligent transport systems applications," *Rec. ITU-R M.2057-1*, 2018.

[5] "Advanced driver assistance systems," *European Commission, Directorate General for Transport*, Nov. 2016.

[6] P. Kumari, J. Choi, N. González-Prelcic, and R. W. Heath, "IEEE 802.11 ad-based radar: An approach to joint vehicular communication-radar system," *IEEE Transactions on Vehicular Technology*, vol. 67, no. 4, pp. 3012–3027, 2017.

[7] D. Solomitckii, V. Semkin, A. Karttunen, V. Petrov, S. Le Hong Nguyen, H. Nikopour, K. Haneda, S. Andreev, S. Talwar, and Y. Koucheryavy, "Characterizing radio wave propagation in urban street canyon with vehicular blockage at 28 GHz," *IEEE Transactions on Vehicular Technology*, Jan. 2020.

[8] R. A. Foran, T. B. Welch, and M. J. Walker, "Very near ground radio frequency propagation measurements and analysis for military applications," in *MILCOM 1999. IEEE Military Communications. Conference Proceedings (Cat. No. 99CH36341)*, vol. 1. IEEE, 1999, pp. 336–340.

[9] H. Klaina, A. Alejos, O. Aghzout, and F. Falcone, "Characterization of near-ground radio propagation channel for wireless sensor network with application in smart agriculture," in *Multidisciplinary Digital Publishing Institute Proceedings*, vol. 2, no. 3, 2017, p. 110.

[10] Y. S. Meng, Y. H. Lee, and B. C. Ng, "Path loss modeling for near-ground VHF radio-wave propagation through forests with tree-canopy reflection effect," *Progress In Electromagnetics Research*, vol. 12, pp. 131–141, 2010.

[11] C. B. Barneto, M. Turunen, S. D. Liyanaarachchi, L. Anttila, A. Brihuega, T. Riihonen, and M. Valkama, "High-accuracy radio sensing in 5G new radio networks: Prospects and self-interference challenge," in *2019 53rd Asilomar Conference on Signals, Systems, and Computers*. IEEE, 2019, pp. 1159–1163.